



Available online at www.sciencedirect.com



Nuclear Physics A 00 (2018) 1–5

**Nuclear
Physics A**

www.elsevier.com/locate/procedia

**XXVIth International Conference on Ultrarelativistic Nucleus-Nucleus Collisions
(Quark Matter 2017)**

Latest results from the EbyE NLO EKRT model

K. J. Eskola^{a,b}, H. Niemi^c, R. Paatelainen^a, K. Tuominen^{d,b}

^a*University of Jyväskylä, Department of Physics, P.O.B. 35, FI-40014 University of Jyväskylä, Finland*

^b*Helsinki Institute of Physics, P.O.B. 64, FI-00014 University of Helsinki, Finland*

^c*Institut für Theoretische Physik, Johann Wolfgang Goethe-Universität, Max-von-Laue-Str. 1, D-60438 Frankfurt am Main, Germany*

^d*Department of Physics, P.O.B. 64, FI-00014 University of Helsinki, Finland*

Abstract

We review the results from the event-by-event next-to-leading order perturbative QCD + saturation + viscous hydrodynamics (EbyE NLO EKRT) model. With a simultaneous analysis of LHC and RHIC bulk observables we systematically constrain the QCD matter shear viscosity-to-entropy ratio $\eta/s(T)$, and test the initial state computation. In particular, we study the centrality dependences of hadronic multiplicities, p_T spectra, flow coefficients, relative elliptic flow fluctuations, and various flow-correlations in 2.76 and 5.02 TeV Pb+Pb collisions at the LHC and 200 GeV Au+Au collisions at RHIC. Overall, our results match remarkably well with the LHC and RHIC measurements, and predictions for the 5.02 TeV LHC run are in an excellent agreement with the data. We probe the applicability of hydrodynamics via the average Knudsen numbers in the space-time evolution of the system and viscous corrections on the freeze-out surface.

Keywords:

heavy-ion collisions, next-to-leading order perturbative QCD calculations, saturation, dissipative fluid dynamics

1. NLO EbyE EKRT model and its tests

The EKRT model [1, 2] rests on the idea that primary particle production in high energy heavy-ion collisions is dominated by few-GeV gluons, minijets [3], whose production rates are computable from collinear factorization of perturbative QCD (pQCD) but controlled by the phenomenon of saturation locally in the transverse plane [4, 5, 6]. The produced minijet densities can then be converted into initial conditions for relativistic fluid dynamics simulations. In NLO pQCD, the infrared- and collinear-safe quantity computed here is the transverse energy E_T carried by the minijets into a mid-rapidity window Δy [7, 5] per transverse area $d^2\mathbf{r}$ in $A+A$ collisions at cms-energy $\sqrt{s_{NN}}$ and impact parameter \mathbf{b} ,

$$\frac{dE_T}{d^2\mathbf{r}}(p_0, \sqrt{s_{NN}}, A, \Delta y, \mathbf{r}, \mathbf{b}; \beta) \stackrel{\text{pQCD}}{=} T_A(\mathbf{r} + \mathbf{b}/2)T_A(\mathbf{r} - \mathbf{b}/2)\sigma\langle E_T \rangle_{p_0, \Delta y, \beta} \stackrel{\text{saturation}}{=} \frac{K_{\text{sat}}}{\pi} p_0^3 \Delta y, \quad (1)$$

where the transverse momentum cut-off $p_0 \sim$ few GeV, and T_A is the nuclear thickness function. The NLO quantity $\sigma\langle E_T \rangle_{p_0, \Delta y, \beta}$ is computed using collinear factorization and the subtraction method [8]. It contains the CTEQ6M parton distributions [9] with EPS09s nuclear effects [10], $2 \rightarrow 3$ and UV-renormalized $2 \rightarrow 2$

parton scattering matrix elements [11], and the measurement functions to define the E_T . The minimum E_T in Δy is controlled by the parameter $\beta \in [0, 1]$, fixed to 0.8 here [5]. Saturation here is the limit where E_T production from $(n > 2) \rightarrow 2$ parton processes starts to dominate over the usual $2 \rightarrow 2$ ones. This can be cast into the form of the saturation condition appearing on the r.h.s. of Eq. (1), where K_{sat} is a free parameter [5]. Equation (1) gives the saturation momentum $p_0 = p_{\text{sat}}(\sqrt{s_{NN}}, A, \mathbf{r}, \mathbf{b}; \beta, K_{\text{sat}})$ locally in the transverse plane. With a formation time $\tau_s(\mathbf{r}) = p_{\text{sat}}(\mathbf{r})^{-1}$ the initial local energy density is then

$$e(\mathbf{r}, \tau_s(\mathbf{r})) = \frac{dE_T}{d^2\mathbf{r}} \frac{1}{\tau_s(\mathbf{r})\Delta y} = \frac{K_{\text{sat}}}{\pi} [p_{\text{sat}}(\mathbf{r})]^4. \quad (2)$$

The key observation [6, 12] enabling the recently developed NLO EbyE EKRT model framework of Ref. [2] is that $p_{\text{sat}}(\mathbf{r}, \mathbf{b}) \approx p_{\text{sat}}(T_A T_A)$ which can be parametrized. Then the T_A s can be made to fluctuate EbyE: we sample the nucleon positions from the standard Woods-Saxon density, setting a Gaussian gluon thickness function of a width $\sigma = 0.43$ fm [14] around each nucleon, and then computing the T_A as a sum of these gluon clouds. Thus, the fluctuations of T_A determine how $e(\mathbf{r}, \tau_s(\mathbf{r}))$ fluctuates here EbyE. Finally, to start our hydro simulations at a constant time, we evolve the e -profile from $\tau_s(\mathbf{r})$ to $\tau_0 = 1/p_{\text{sat}}^{\min} = 0.2$ fm using 0+1 D Bjorken hydrodynamics. At the edges of the system, we assume a binary e -profile.

With such initial conditions, we describe the spacetime evolution of produced QCD matter then EbyE, using 2nd-order dissipative relativistic 2+1 D hydro with transient fluid-dynamics equation of motion for the shear-stress tensor $\pi^{\mu\nu}$ from Refs. [15, 16]. The transverse flow and $\pi^{\mu\nu}$ are initially zero. Our equation of state is s95p-PCE-v1 [17], with chemical decoupling at $T_{\text{chem}} = 175$ MeV. Kinetic freeze-out is at $T_{\text{dec}} = 100$ MeV, and on this surface we assume, as usual, that the viscous δf -corrections are $\propto p_\mu p_\nu \pi^{\mu\nu}$. We neglect the bulk viscosity and heat conductivity. We study the T dependence of $\eta/s(T)$ with the parametrizations of Fig. 1a, all of which are designed to reproduce the flow coefficients $v_n\{2\}$ measured in 2.76 TeV Pb+Pb collisions at the LHC, as shown in Fig. 1b. The parameter K_{sat} is fixed separately for each $\eta/s(T)$ parametrization, by using the $dN_{\text{ch}}/d\eta(0 - 5\%)$ measured by ALICE in 2.76 TeV Pb+Pb collisions (Fig. 3a).

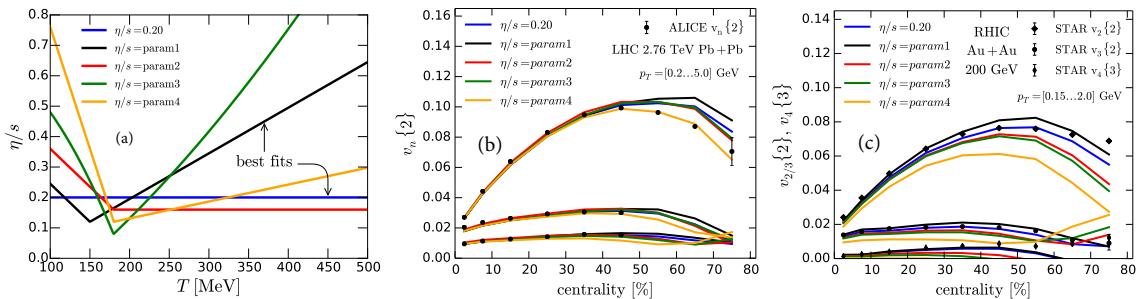


Fig. 1. (a) The tested $\eta/s(T)$ parametrizations. Flow coefficients $v_n\{2\}$ vs. ALICE data [18] in 2.76 TeV Pb+Pb collisions at the LHC (b), and $v_2\{2\}$, $v_3\{2\}$ and $v_4\{3\}$ vs. STAR data [19, 20, 21] in 200 GeV Au+Au collisions (c). From [13, 2].

We have extensively tested the NLO EbyE EKRT model in [2], arriving at a very good simultaneous description of the centrality dependences of charged hadron multiplicities, p_T spectra, and flow coefficients in 2.76 TeV Pb+Pb collisions at the LHC and 200 GeV Au+Au at RHIC. As seen in Fig. 1c, the RHIC v_n s favor 0.2 (blue) and *param1* (black) for $\eta/s(T)$. Also the correlations of 2 and 3 event-plane angles measured by ATLAS systematically favor these two $\eta/s(T)$ parametrizations, see Fig. 2a [2]. Furthermore, these constraints are obtained in the centrality region where the δf effects remain small in these observables [2]. Relative EbyE fluctuations of v_2 measured by ATLAS provide a stringent η/s -independent test for the computed initial states. The EKRT model passes also this test remarkably well, demonstrating the necessity of a hydro evolution in understanding the centrality systematics of this observable [2].

As a measure of our hydro validity, we plot in Fig. 2f also (i) the average Knudsen numbers $\langle \text{Kn} \rangle$, expansion rate ($\theta = \partial_\mu u^\mu$) per thermalization time ($\tau_\pi = 5\eta/(e+p)$) averaged over entropy density throughout the evolution ($T > 100$ MeV), and (ii) the shear stress over pressure ($\sqrt{\pi_{\mu\nu}\pi^{\mu\nu}/p}$) averaged over the entropy flux through the freeze-out surface. This reflects the average δf corrections in the end of the evolution. The

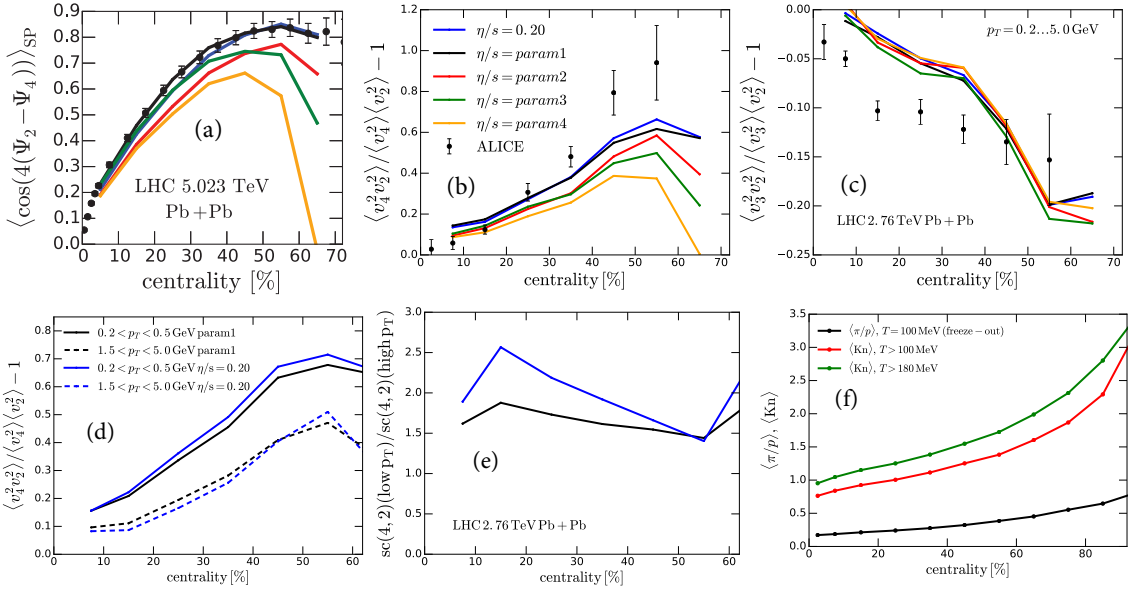


Fig. 2. Centrality dependence of various correlators and Knudsen number in 2.76 TeV Pb+Pb collisions. (a) Correlation of the event-plane angles Ψ_2 and Ψ_4 vs. ATLAS data [23]. From [2]. (b) Normalized cumulants $SC(4,2)/\langle v_4^2 \rangle \langle v_2^2 \rangle$ vs. ALICE data [24]. (c) Same for $SC(3,2)/\langle v_3^2 \rangle \langle v_2^2 \rangle$. (d) $SC(4,2)/\langle v_4^2 \rangle \langle v_2^2 \rangle$ in one low- p_T and one high- p_T interval, computed with our two best-fit η/s parametrizations. (e) Low-to-high- p_T ratio of $SC(4,2)/\langle v_4^2 \rangle \langle v_2^2 \rangle$. (f) Average Knudsen numbers $\langle Kn \rangle$ in our hydro evolution (red, green), and average shear stress over pressure $\langle \pi/p \rangle$ on the freeze-out surface (black), computed with the $param1$ η/s parametrization.

facts that these indicators increase towards peripheral collisions only gradually and that $\langle Kn \rangle = O(1)$ speak for the hydro validity at least up to 50% centralities. Towards peripheral collisions, $\langle Kn \rangle$ increases due to the increasing relative weight of the early stages where $\langle Kn \rangle$ is large (see the $T > 180$ MeV curve).

2. Further predictions from the EbyE NLO EKRT model

We have made a series of predictions from the EbyE NLO EKRT model without any further tuning. For ALICE, we have computed the symmetric 2-harmonic 4-particle cumulants, $SC(m, n) = \langle \langle \cos(m\phi_1 + n\phi_2 - m\phi_3 - n\phi_4) \rangle \rangle = \langle v_m^2 v_n^2 \rangle - \langle v_m^2 \rangle \langle v_n^2 \rangle$ normalized by $\langle v_m^2 \rangle \langle v_n^2 \rangle$ shown in Fig. 2b,c. Our best-fit η/s parametrizations predict rather well the positive correlation seen by ALICE [24] in $SC(4, 2)$ and also the trend of the negative correlation in $SC(3, 2)$. We emphasize, however, the importance of a 1-to-1 comparison: we expect that once we include the multiplicity weighting assumed in the ALICE analysis, our prediction will be systematically closer to the data. In Fig. 2d we show a prediction of the p_T dependence of $SC(4, 2)/\langle v_4^2 \rangle \langle v_2^2 \rangle$. Fig. 2e in turn suggests that the low-to-high- p_T ratios of these normalized correlators might be able to distinguish between our best-fit η/s parametrizations. Similarly, we have provided the STAR collaboration with our predictions for the centrality dependence of mixed harmonic correlators $C_{m,n,m+n} = \langle \langle \cos(m\phi_1 + n\phi_2 - (m+n)\phi_3) \rangle \rangle$. As shown in [22], our best-fit parametrizations reproduce the $C_{2,2,4}$ rather well. However, we underestimate the measured $C_{2,3,5}$, which we believe is due to large δf effects in this observable, possibly combined also with non-flow and rapidity effects which we cannot consider, yet. Further studies on this are ongoing.

Thanks to the predictive power of the EKRT model, we have also made predictions for the 5.02 TeV Pb+Pb run at the LHC [13]. Figure 3 shows our predictions for the multiplicity and flow-coefficient ratios. In the latter, notice the slight increase with increasing n . Again, as seen in the figure, the EbyE NLO EKRT model fairs very well in the data comparison.

To conclude, the EbyE NLO EKRT model [2] explains consistently the bulk observables and various correlators at mid-rapidity in LHC and RHIC heavy-ion collisions. Its predictive power in cms-energy, centrality and nuclear mass number has been demonstrated with various observables. Via a multi-energy and multi-observable analysis we have managed to constrain the $\eta/s(T)$ ratio, for which two best-fit parametrizations have been identified. Similar results have been found also in Ref. [31]. Systematic further tests of the

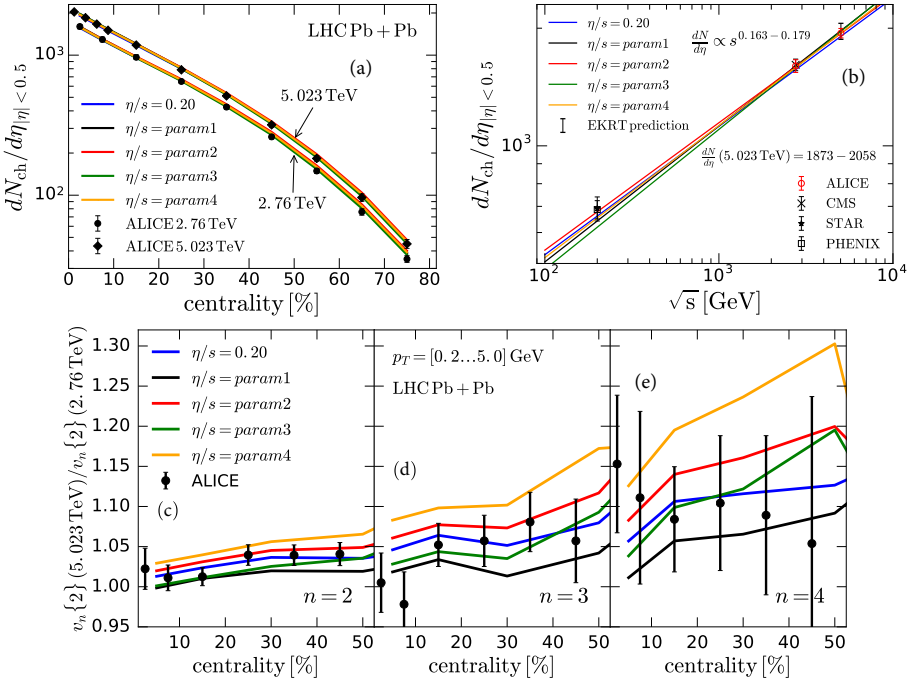


Fig. 3. EbyE NLO EKRT model predictions for 5.023 TeV Pb+Pb collisions [13]. (a) Centrality dependence of charged particle multiplicity, vs. ALICE data [25, 26]. (b) Predicted $\sqrt{s_{NN}}$ dependence of charged particle multiplicity from RHIC Au+Au to LHC Pb+Pb collisions vs. data from ALICE [25, 26], CMS [27], STAR [28] and PHENIX [29]. (c-e) Ratio of the flow coefficients $v_n(2)$ in 5.023 TeV and 2.76 TeV Pb+Pb collisions, vs. ALICE data [30].

hydro results validity are, however still needed, especially in the case of more complicated correlators, as well as more work for including further dissipative phenomena.

Acknowledgments. K.J.E. is supported by the Academy of Finland, Project 297058, and H.N. by the EU's Horizon 2020 research and innovation programme under the Marie Skłodowska-Curie grant agreement no. 655285.

References

- [1] K. J. Eskola, K. Kajantie, P. V. Ruuskanen and K. Tuominen, Nucl. Phys. B **570**, 379 (2000) [hep-ph/9909456].
- [2] H. Niemi, K. J. Eskola and R. Paatelainen, Phys. Rev. C **93** (2016) no.2, 024907 [arXiv:1505.02677 [hep-ph]].
- [3] K. J. Eskola, K. Kajantie and J. Lindfors, Nucl. Phys. B **323** (1989) 37.
- [4] K. J. Eskola, K. Kajantie and K. Tuominen, Phys. Lett. B **497** (2001) 39 [hep-ph/0009246].
- [5] R. Paatelainen, K. J. Eskola, H. Holopainen and K. Tuominen, Phys. Rev. C **87**, no. 4, 044904 (2013) [arXiv:1211.0461 [hep-ph]].
- [6] R. Paatelainen, K. J. Eskola, H. Niemi and K. Tuominen, Phys. Lett. B **731**, 126 (2014) [arXiv:1310.3105 [hep-ph]].
- [7] K.J. Eskola and K. Tuominen, Phys. Lett. B **489** (2000) 329 [hep-ph/0002008]; Phys. Rev. D **63** (2001) 114006 [hep-ph/0010319].
- [8] Z. Kunszt and D. E. Soper, Phys. Rev. D **46** (1992) 192.
- [9] J. Pumplin, D. R. Stump, J. Huston, H. L. Lai, P. M. Nadolsky and W. K. Tung, JHEP **0207** (2002) 012 [hep-ph/0201195].
- [10] I. Helenius, K. J. Eskola, H. Honkanen and C. A. Salgado, JHEP **1207**, 073 (2012) [arXiv:1205.5359 [hep-ph]].
- [11] R. K. Ellis and J. C. Sexton, Nucl. Phys. B **269**, 445 (1986); R. Paatelainen, PhD thesis, arXiv:1409.3508 [hep-ph].
- [12] K. J. Eskola, K. Kajantie and K. Tuominen, Nucl. Phys. A **700**, 509 (2002) [hep-ph/0106330].
- [13] H. Niemi, K. J. Eskola, R. Paatelainen and K. Tuominen, Phys. Rev. C **93** (2016) no.1, 014912 [arXiv:1511.04296 [hep-ph]].
- [14] S. Chekanov *et al.* [ZEUS Collaboration], Nucl. Phys. B **695**, 3 (2004) [hep-ex/0404008].
- [15] G. S. Denicol *et al.*, Phys. Rev. D **85**, 114047 (2012) [Phys. Rev. D **91**, no. 3, 039902 (2015)] [arXiv:1202.4551 [nucl-th]].
- [16] E. Molnár, H. Niemi, G. S. Denicol and D. H. Rischke, Phys. Rev. D **89**, no. 7, 074010 (2014) [arXiv:1308.0785 [nucl-th]].
- [17] P. Huovinen and P. Petreczky, Nucl. Phys. A **837**, 26 (2010) [arXiv:0912.2541 [hep-ph]].
- [18] K. Aamodt *et al.* [ALICE Collaboration], Phys. Rev. Lett. **107**, 032301 (2011) [arXiv:1105.3865 [nucl-ex]].
- [19] J. Adams *et al.* [STAR Collaboration], Phys. Rev. C **72**, 014904 (2005) [nucl-ex/0409033].
- [20] L. Adamczyk *et al.* [STAR Collaboration], Phys. Rev. C **88**, no. 1, 014904 (2013) [arXiv:1301.2187 [nucl-ex]].
- [21] J. Adams *et al.* [STAR Collaboration], Phys. Rev. Lett. **92**, 062301 (2004) [nucl-ex/0310029].
- [22] L. Adamczyk *et al.* [STAR Collaboration], arXiv:1701.06497 [nucl-ex].
- [23] G. Aad *et al.* [ATLAS Collaboration], Phys. Rev. C **90**, no. 2, 024905 (2014) [arXiv:1403.0489 [hep-ex]].

- [24] J. Adam *et al.* [ALICE Collaboration], Phys. Rev. Lett. **117** (2016) 182301 [arXiv:1604.07663 [nucl-ex]].
- [25] K. Aamodt *et al.* [ALICE Collaboration], Phys. Rev. Lett. **106**, 032301 (2011) [arXiv:1012.1657 [nucl-ex]].
- [26] J. Adam *et al.* [ALICE Collaboration], Phys. Rev. Lett. **116** (2016) no.22, 222302 [arXiv:1512.06104 [nucl-ex]].
- [27] S. Chatrchyan *et al.* [CMS Collaboration], JHEP **1108** (2011) 141 [arXiv:1107.4800 [nucl-ex]].
- [28] B. I. Abelev *et al.* [STAR Collaboration], Phys. Rev. C **79** (2009) 034909 [arXiv:0808.2041 [nucl-ex]].
- [29] S.S. Adler *et al.* [PHENIX Collab.], Phys. Rev. C **71** (2005) 034908 Erratum: [Phys. Rev. C **71** (2005) 049901] [nucl-ex/0409015].
- [30] J. Adam *et al.* [ALICE Collaboration], Phys. Rev. Lett. **116** (2016) no.13, 132302 [arXiv:1602.01119 [nucl-ex]].
- [31] J. E. Bernhard *et al.*, Phys. Rev. C **94** (2016) no.2, 024907 [arXiv:1605.03954 [nucl-th]].